

Influence of Nitrogen Content on Zirconophosphate Oxynitrides Acid–Base Properties

N. Fripiat,* R. Conanec,† A. Auroux,‡ Y. Laurent,† and P. Grange*

*Université Catholique de Louvain, Place Croix du Sud 2/17, 1348 Louvain-la-Neuve, Belgium; †Université de Rennes I, Avenue Général Leclerc, 35042 Rennes Cedex, France; and ‡Institut de Recherche sur la Catalyse, CNRS, 2 Avenue Albert Einstein, 69626 Villeurbanne Cedex, France

Received October 21, 1996; revised January 6, 1997; accepted January 6, 1997

A new family of phosphate oxynitrides was prepared by nitridation of an amorphous zirconophosphate precursor under ammonia flow. The oxygen substitution by nitrogen modified the acid–base properties of the zirconophosphate oxynitrides obtained. Surface acidity decreased sharply when bulk nitrogen content increased while basic properties as measured by SO_2 adsorption calorimetry greatly depended on the O/N ratio. At 50°C, the Knoevenagel condensation of benzaldehyde with malononitrile in toluene brings an 80% of conversion after 5 h. © 1997 Academic Press

1. INTRODUCTION

Several studies have addressed the acidic properties of crystalline zirconium phosphates and their use as solid acid catalysts. Two types of acid sites with different acid strengths have been found on these surfaces (1): strong acid sites due to residual P–OH groups remaining on the surface, and weak acid sites as interlayer P–OH groups. Zirconophosphate compounds were successfully employed for alcohol dehydration (2–5), oxidative dehydrogenation (6), partial oxidation (6), and polymerization reactions (6). They can also catalyze MTBE formation from methanol and isobutene with high selectivities (7). On the other hand, relatively little attention has been paid to the importance of basic sites in catalysis with phosphates, although there has been a growing interest in base-catalyzed processes in fine chemistry in the past few years (8).

We have shown recently that incorporation of nitrogen in the anionic network of aluminophosphate is an effective way to modify the surface acid–base properties of phosphate compounds and particularly to increase surface basicity (9–13). This new family of amorphous aluminophosphate oxynitrides (AlPON) has been synthesized thanks to a method of nitride preparation using a temperature-programmed nitridation of an oxide precursor in a stream of ammonia (14–16). The resulting AlPON solids maintain the very high specific surface area of the precursor. This original synthetic method can be extended to the preparation of other oxynitride systems such as aluminum–

gallium–phosphorus–oxygen–nitrogen (AlGaPON) (17), zirconium–phosphorus–oxygen–nitrogen (ZrPON) (18) or vanadium–aluminum–oxygen–nitrogen (VALON) (19). It has been reported in a previous paper (18) that nitrogen present in oxynitride zirconium phosphate modifies the acid–base properties of this solid and enhances basic catalyzed reactions such as Knoevenagel condensation. Compared to MgO , a commercial basic catalyst, the ZrPON catalyst shows a remarkably higher activity.

This work reports on the physicochemical characterization of a series of zirconophosphate oxynitrides (ZrPON) with variable nitrogen content and shows the possibility of tuning their surface basicity.

2. METHODS

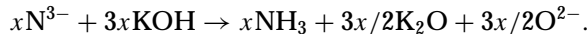
2.1. Materials

The citrate method (20) was used to prepare the high-surface-area amorphous phosphate precursor. Twenty grams of $\text{ZrO}(\text{NO}_3)_2 \cdot 3,4\text{H}_2\text{O}$ (Acros Chimica, 99.5%) was dissolved by slight heating in 250 ml of distilled water. Twenty milliliters of a 0.37 M (H_3PO_4) (Fluka) solution was then added. The Zr/P atomic ratio was fixed at 0.9. After stirring for 1 h, an excess of citric acid (Merck, p.a., 55 g) was added to the viscous and gelatinous precipitate. The resulting product was further stirred overnight. Water was then evaporated under reduced pressure and the precipitate was dried for 20 h at 120°C under vacuum (5×10^3 Pa). The sample was then calcined for 16 h at 500°C. Nitridation of the phosphate precursor was carried out under flowing pure ammonia. Various nitrogen contents were obtained by modification of both nitridation time and temperature within the range of 0.75 to 73 h and 590 to 790°C, respectively (21). At the end of the activation process, the samples were allowed to cool to room temperature under a pure and dry nitrogen flow.

2.2. Nitrogen Content of Solids

The principle of the determination of the total nitrogen content was based on the displacement reaction of nitride

ions N^{3-} induced by an excess of strong base, which leads to the formation of ammonia (22). The zirconophosphate oxynitride was attacked at 400°C with melted potassium hydroxide under inert atmosphere:



The ammonia was dissolved in water and titrated with a sulfuric acid solution.

2.3. X-Ray Diffraction and Surface Area Analysis

X-ray diffraction of samples was carried out in a Siemens D-5000 powder diffractometer using Ni-filtered $\text{CuK}\alpha 1$ radiation ($\lambda = 1.5406 \text{ \AA}$).

The specific surface area was measured by the single-point BET method ($p/p_0 = 0.3$) in a Micromeritics Flowsorb 2000 apparatus. Samples were degassed for 1 h at 150°C under nitrogen flow before analysis at liquid nitrogen temperature.

2.4. FTIR Analysis

Pyridine absorption spectra were recorded using a Brücker IFS 88 FTIR spectrometer in the 4000–400 cm^{-1} range with 2 cm^{-1} resolution. The powders were pressed into self-supporting disks (10 mg, 13 mm in diameter) and placed inside an IR cell connected to a vacuum line allowing *in situ* experiments at temperatures up to 450°C under vacuum or under controlled atmosphere. The wafers were degassed under vacuum before analyses at 400°C for 1 h. Pyridine was then introduced at room temperature. After evacuation of the sample, the free and physisorbed species have disappeared and only chemisorbed species remained on the surface. These species were desorbed with increasing temperature (100, 200, and 300°C) under vacuum.

2.5. Ammonia Chemisorption Analysis

Ammonia chemisorption experiments were performed at different temperatures (30, 100, and 200°C) using a static volumetric apparatus (Micromeritics ASAP 2010C adsorption analyzer). The samples (0.1 g) were previously degassed at 400°C for 2 h at 10⁻¹ Pa. In order to differentiate between ammonia physisorption and chemisorption, all analyses were repeated after the initial adsorption. The samples were degassed at the analysis temperature for 0.5 h between both analyses. In this work, only the ammonia chemisorption results are presented.

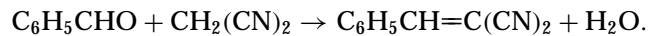
2.6. Adsorption Microcalorimetry of SO_2

Sulfur dioxide ($\text{p}K_a$ 1.89) was chosen as a probe molecule to perform calorimetric and volumetric gas–solid titration of the basic sites of the samples. Sulfur dioxide (Air Liquide, purity >99.9%) was purified by successive freeze–thaw cycles before use. The differential heats of adsorption of sul-

fur dioxide were measured by a heat-flow microcalorimeter (Setaram C80) linked to a volumetric adsorption system, at 80°C. The sample, weighing about 100 mg, was heated in the calorimetric cell to 300°C at the rate of 1°C · min⁻¹ and maintained for 8 h at this temperature under 10⁻⁴ Pa and then placed in the calorimeter. Successive small doses of the adsorbate (SO_2) were passed over the catalyst. The adsorbed amount and the heat released were determined simultaneously at every coverage. The pressure was measured by means of a transducer gauge (Barocel Datametrics) which enabled accurate measurements of equilibrium pressure up to about 133 Pa. Both the calorimetric and the volumetric data were stored and analyzed by microcomputer processing. Furthermore, in order to calculate the irreversibly chemisorbed amount (V_{irr}), the sample was pumped at 80°C at the end of the adsorption, and a secondary adsorption was then performed at the same temperature. V_{irr} was determined from the difference between the primary and the secondary isotherms.

2.7. Catalytic Evaluation

The zirconophosphate oxynitride basicity was also estimated by using the Knoevenagel reaction which consists in the condensation of benzaldehyde with malononitrile.



Four micromoles of each reactant and 30 ml of toluene as solvent were introduced in a 50-ml flask equipped with a magnetic stirrer and heated at 50°C. Then, 0.05 g of catalyst was added to the solution. Liquid samples were regularly withdrawn with a filtering syringe and analyzed by a gas chromatograph (Intersmat Delsi Di 200), equipped with an FID detector and using a capillary column (CPSil8CB, 25 m).

3. RESULTS AND DISCUSSION

3.1. Composition and Morphology

The nitridation process under flowing pure ammonia of the amorphous and high-surface-area precursor (ZrPO) leads to the formation of zirconophosphate oxynitrides with variable N contents (Table 1). The N content permits the establishment of the global composition of these new solids, assuming that the electroneutrality and Zr/P atomic ratio of starting zirconophosphate are maintained after oxygen to nitrogen substitution. These compositions may be represented as $\text{Zr}_{0.9}\text{PO}_{4.3-3x/2}\text{N}_x$. Note that the surface area remained high (>100 m^2/g) after heating in spite of various unfavorable factors such as high reaction temperature, thermal treatment time, chemical composition modification, and water production during nitridation, which is known to induce sintering. All the samples (precursor and nitrided samples) are X-ray amorphous.

TABLE 1

Chemical Compositions and Specific Surface Areas of the Precursor ZrPO and Zirconophosphate Oxynitrides (ZrPON)

Sample	Nitridation		N content (wt%)	Composition	Surface area (m ² /g)
	Time (h)	T (°C)			
ZrPO	—	—	0	Zr _{0.90} PO _{4.30}	230
ZrPON1	0.75	590	1.8	Zr _{0.90} PO _{3.95} N _{0.23}	210
ZrPON2	0.50	790	5.4	Zr _{0.90} PO _{3.29} N _{0.68}	155
ZrPON3	12.75	700	8.2	Zr _{0.90} PO _{2.79} N _{1.01}	180
ZrPON4	14.25	750	11.2	Zr _{0.90} PO _{2.28} N _{1.35}	135
ZrPON5	73	790	19	Zr _{0.90} PO _{1.04} N _{2.18}	115

3.2. Structural Analysis

Some FTIR peaks due to the presence of amine and hydroxyl functions could be observed after water desorption by pretreatment of the samples at 400°C under 10⁻⁴ Pa for 1 h (Fig. 1). The sharp peak located at 3671 cm⁻¹ is assigned to a vibrational mode of OH groups linked to phosphorus atoms ($\nu_{\text{PO}-\text{H}}$) (23), while the weak peak around 3763 cm⁻¹ is attributed to a vibrational mode of OH groups linked to zirconia atoms ($\nu_{\text{ZrO}-\text{H}}$) (24). The large band centred around 3320 cm⁻¹ is due to a stretching mode of NH_x species (25). When the N content increases, the relative intensities of the $\nu_{\text{PO}-\text{H}}$ and $\nu_{\text{ZrO}-\text{H}}$ bands decrease, meaning that hydroxyl species at the surface are replaced by NH_x species during the nitridation process. In the 1800 to 1400 cm⁻¹ spectral area, different vibrational bands are observed depending on the pretreatment temperature (Fig. 2). When powders were degassed at 250°C under 10⁻⁴ Pa (Fig. 2A), two spectral bands at 1630 and 1430 cm⁻¹ were observed for samples with low N content. These can be assigned, respectively, to the bending deformation $\delta_{\text{N}-\text{H}}$ mode of NH₂

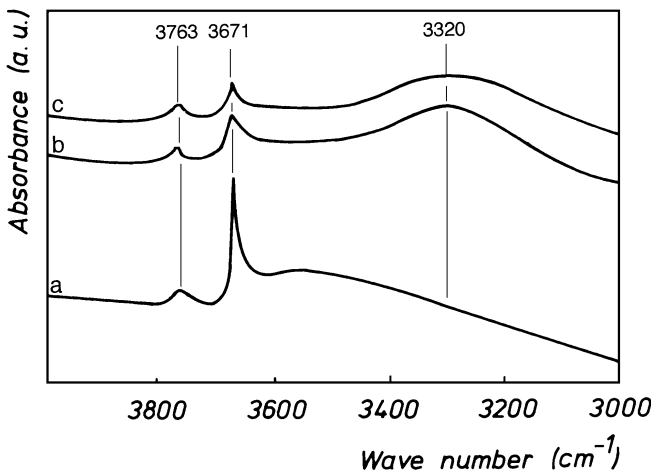


FIG. 1. IR spectra of ZrPON oxynitrides with various bulk N content: 0% (a), 8.2% (b) and 19% (c).

or NH₃ and to ammonium species adsorbed at the solid surface. This last band disappears completely when the pretreatment temperature increases to 400°C, while a new peak appears around 1550 cm⁻¹ due to the bending vibrational frequency of a new P-NH₂ species (25) (Fig. 2B). At high N content, only this peak is observed.

From this analysis, it can be deduced that nitrogen is present preferentially in the coordination sphere of phosphorus, since a decrease of $\nu_{\text{P}-\text{OH}}$ and creation of new P-N bonds are observed while N content increases. No evidence has been found for the presence of Zr-N bonds. For low N contents, many adsorbed species (NH₃, NH₄⁺) are removed by heating, leading to the formation of new P-NH₂ bonds.

3.3. Acid Properties

The acid properties of the solids have been evidenced by FTIR with pyridine adsorption and ammonia chemisorption. The results of these analyses show that the presence of nitrogen in the phosphate structure modifies both the number and strength of the acid sites of these solid powders.

3.3.1. FTIR study with pyridine adsorption. Pyridine adsorbed on an acidic surface can react in two ways, depending upon the type of site. On Lewis acid sites, some coordination bonds are formed which give rise to bands near 1620–1600 cm⁻¹ (ν_{8a}) and 1450 cm⁻¹ (ν_{19b}), while protonation on Brønsted sites gives characteristic bands at 1640 and 1540 cm⁻¹ (26, 27). The ν_{8a} wave number is representative of the strength of the Lewis acid sites, while the intensity of the ν_{19b} band characterizes their number.

The adsorption of pyridine at room temperature results in the formation of coordination bonds on Lewis acid sites (Fig. 3). Pyridinium ions also seem to be present, but the band width does not permit any further quantification. From Fig. 4, it appears that the total number of Lewis acid sites per gram (area of ν_{19b} normalized by the weight of the pellets) is higher on the precursor and that it sharply decreases as soon as nitrogen is present. This curve suggests that the nitridation process involves the departure of oxygen species (O²⁻ or OH⁻) which are linked to surface acidity. These species are strongly exchanged until the N content reaches 5 wt%. When the desorption temperature increases, the number of Lewis acid sites decreases whatever the N content. Only the precursor surface still possesses a significant quantity of adsorb pyridine after degassing at 300°C. A shift of the ν_{8a} band toward higher energy is observed, which means that only stronger sites remain on the surface at this temperature. It can be concluded that the phosphate precursor is more acidic than nitrided samples and that ZrPON with a N content higher than 1.8 wt% possesses very few strong acid sites. It is suggested that this evolution can be explained by the difference in electronegativity between oxygen and nitrogen since nitrogen is less electronegative than oxygen, the O/N substitution

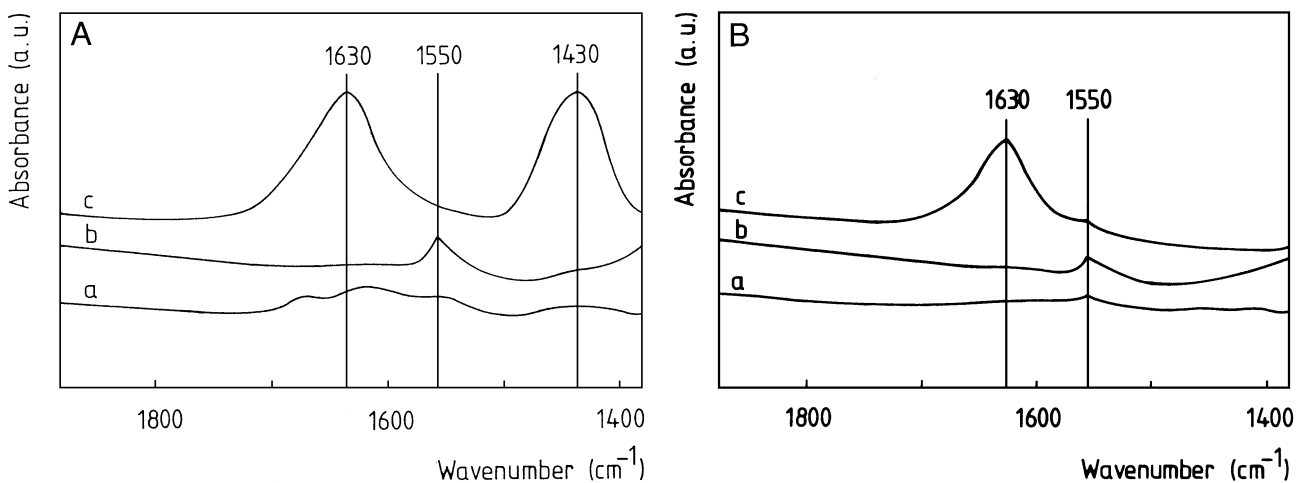


FIG. 2. (A) IR spectra of ZrPON oxynitrides pretreated at 250°C. ZrPO (0 wt% N) (a); ZrPON3 (8.2 wt% N) (b); and ZrPON1 (1.8 wt% N) (c). (B) IR spectra of ZrPON oxynitrides pretreated at 400°C. ZrPO (0 wt% N) (a); ZrPON3 (8.2 wt% N) (b); and ZrPON1 (1.8 wt% N) (c).

in the coordination sphere of the cations will reduce their tendency to attract electrons, which results in a decrease of their Lewis acidity.

3.3.2. Ammonia chemisorption analysis. Chemisorption of ammonia is another way to evaluate the surface acidity of a sample (28). The isotherms of ammonia chemisorption are kept at three different temperatures (35, 100, and 200°C). For a given pressure, each point of the isotherm at 35°C lies above the corresponding one at 100°C, which itself lies above the corresponding one at 200°C. This is in agreement with thermodynamics, as ammonia chemisorption is less favored at higher temperature, being an exothermic reaction. It was possible to make rough comparisons among the solids about the number of acid sites directly from the isotherms. These comparisons must be performed at a given pressure. At a given pressure and temperature,

the chemisorbed volume which corresponds to the surface acidity decreases when the N content increases (Fig. 5). The trend observed in FTIR in the adsorption of pyridine is also noticed with this method: the number of acid sites is higher on the precursor and decreases sharply as soon as nitrogen is present. Some information about acidic strength can also be deduced from these analyses when it is considered that only strong sites are able to retain ammonia at 200°C, while the measured volumes at 35 and 100°C correspond, respectively, to the ammonia adsorbed on all sites (weak, medium, and strong) and on the medium and strong sites. The different volumes corresponding to each strength can be found by suitable subtraction (Fig. 5). It appears that the number of strong sites decreases by 50% when 1.8% nitrogen is introduced into the catalyst while medium sites remain virtually constant and weak acid sites decrease by

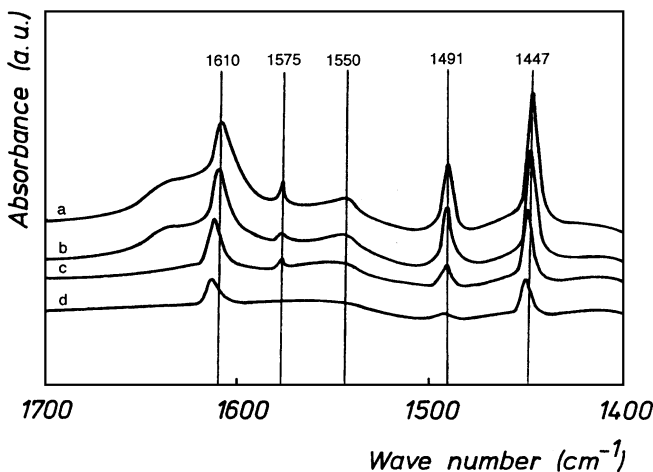


FIG. 3. IR spectra of pyridine adsorbed on ZrPO precursor after evacuation at room temperature (a), 100°C (b), 200°C (c), and 300°C (d).

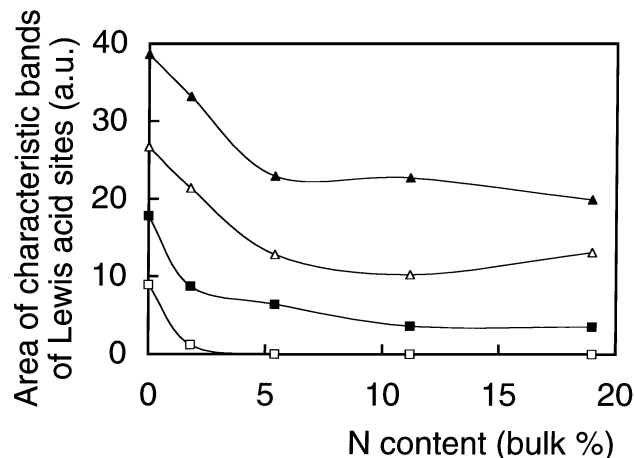


FIG. 4. Area variation of bands characteristic of the total number of Lewis acid sites with various bulk nitrogen contents after evacuation at 20°C (▲), 100°C (△), 200°C (■), and 300°C (□).

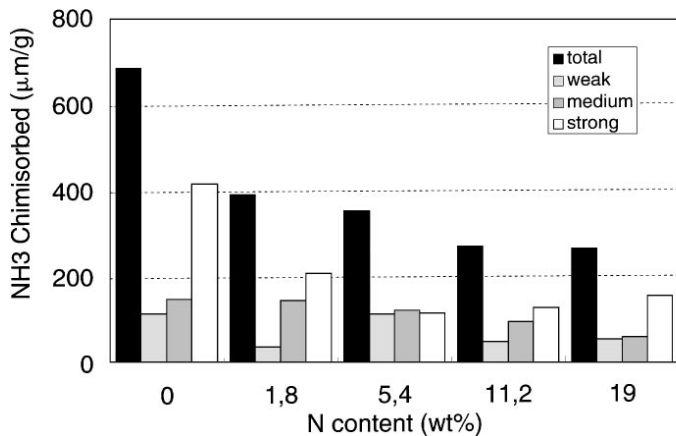


FIG. 5. Total, weak, medium, and strong acid sites repartition measured by ammonia chemisorption versus bulk nitrogen content.

66%. The same tendency is observed with lower intensity when the nitrogen content is increased up to 20%.

3.4. Basic Properties

Sulfur dioxide was chosen as basicity probe molecule in microcalorimetry measurements. The Knoevenagel condensation was also performed as test reaction to evaluate the basic properties of the ZrPON series.

3.4.1. Adsorption calorimetry of SO_2 . The differential molar heats of adsorption on ZrPON samples with the sorbed amount of sulfur dioxide are plotted in Fig. 6. The relatively high initial heats of adsorption observed at low coverage decrease continuously by variable steepness to reach values slightly higher than the heat of liquefaction of SO_2 ($\Delta H^\circ = 18.6 \text{ kJ/mol}$). A wide plateau localized around 150 kJ/mol is observed for the higher N content (ZrPON5), which is representative of the increasing site homogeneity. The heats at zero coverage increase from 130 to 160 kJ/mol for precursor and ZrPON5 (19 wt% N), respectively, which means that increasing the N/O ratio results in an increase of basic strength. These high values could be attributed to the

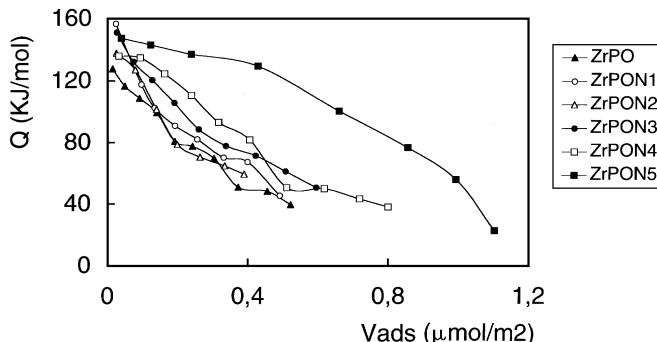


FIG. 6. Differential molar heats of adsorption on ZrPON series versus the adsorbed amount of SO_2 .

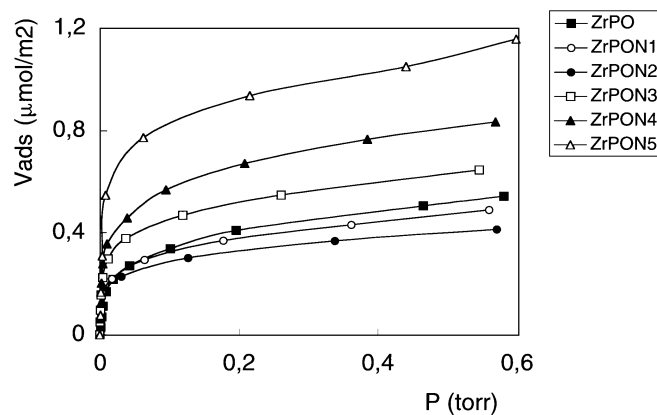


FIG. 7. Adsorption isotherms of SO_2 at 80°C .

SO_2 dipole interactions with the electrostatic field induced by the N^{3-} anions. If one considers the primary adsorption isotherms (Fig. 7), it appears that the addition of 1.8 to 5.4 wt% of nitrogen has only very little influence on the total adsorbed SO_2 amount, which slightly decreases. However, the samples containing 8.2 wt% or more display larger and larger increases in the adsorbed volumes.

Figure 8 represents the total number of sites which adsorb SO_2 at a pressure of 27 Pa as a function of the nitrogen weight loading of the samples, as well as the number of sites (V_{irr}) computed at the same pressure and previously described under Methods. The two curves are parallel, which proves that the number of weak sites remains constant for all samples and that only the strong sites vary. This graph also shows that the initial number of strong sites on the ZrPO sample (about $0.2 \mu\text{mol}/\text{m}^2$), obviously not attributed to nitrogen, can be associated to basic framework oxygen. The stronger basicity of nitrogen compared to oxygen becomes predominant only above about 7 wt% and then increases almost linearly with the nitrogen

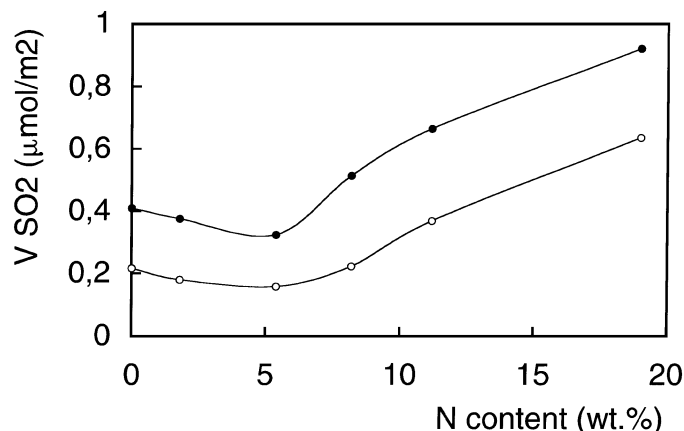


FIG. 8. Variation of total (●) and irreversible (○) volume of SO_2 with bulk nitrogen content.

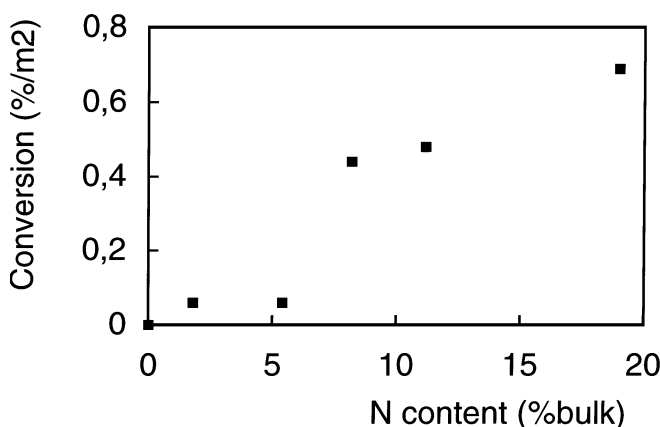


FIG. 9. Variation of conversion after 5 h in Knoevenagel condensation with bulk nitrogen content.

content. The increase in oxynitride basicity is directly linked to the O/N ratio which can be adjusted during the nitridation process. Although the nature of the basic centers is not yet exactly known, it has already been shown that substitution of oxygen by nitrogen gives rise to the formation of N^{3-} , $-\text{NH}-$, or $-\text{NH}_2$ species in SiON (29). On ZrPON, these species correspond to bulk (N^{3-}) and to surface ($-\text{NH}-$ and $-\text{NH}_2$) nitrogen evidenced by FTIR.

3.4.2. Catalytic evaluation. The Knoevenagel condensation of benzaldehyde with malononitrile has been performed as an alternative way of basic properties determination. This type of reaction is often described in the literature as requiring basic sites (30). No activity was found for ZrPO tested under the conditions described above, and the same reaction performed with ZrPON brings 80% conversion after 5 h. It should be noted that any special care (for example, thermal activation) is taken before starting the reaction. Catalytic activity is therefore largely influenced by the N content and surface area which can be adjusted during the preparation step. The evolution of intrinsic conversion rate (%/m^2) versus N content is shown in Fig. 9. Basic properties of zirconium oxynitrides are directly linked to their resources in nitrogen, as conversion rate increases with N content. This last graph must be compared to Fig. 8 which displays a similar trend: the number of basic sites is slightly decreasing for N weight loading of 1.8 to 5.4% while the activity for condensation is constant. When the nitrogen content is greater than 5.4%, the number of basic sites and the conversion increase sharply. The catalytic activity enhancement can thus be related to the increasing number of basic sites rather than to an increase of their strength.

4. CONCLUSION

A new family of amorphous and high-surface-area phosphate oxynitride catalysts have been prepared by temperature-programmed reactions between oxide precursors and ammonia. The influence of nitrogen on surface characteristics and acid-base properties was demonstrated. It is suggested that nitrogen is located in the coordination sphere of phosphorus since zirconium–nitrogen bonds were not observed. FTIR studies with pyridine adsorption and ammonia chemisorption analyses revealed the same acidity trend: the number of acid sites is higher on the precursor surface and sharply decreases as soon as nitrogen is incorporated. The microcalorimetry of SO_2 adsorption and the Knoevenagel condensation of benzaldehyde with malononitrile permitted the evaluation of the basic properties of ZrPON solids: both the number and the strength of the basic sites increase with nitrogen content. It appeared that the condensation rate is linked to the number of basic sites, which itself is a function of nitride nitrogen content adjusted during the preparation step. It is thus possible to tune the acid-base properties in this new family of catalysts by modifying the O/N ratio.

ACKNOWLEDGMENTS

N.F. thanks the FRIA for her grant. We acknowledge the financial support of the “Région Wallonne,” Belgium.

REFERENCES

- Hattori, T., Ishiguro, A., and Murakami, Y., *J. Inorg. Nucl. Chem.* **40**, 1107 (1978).
- Clearfield, A., and Thakur, D. S., *J. Catal.* **65**, 185 (1980).
- Hattori, T., Ishiguro, A., and Murakami, Y., *Nippon Kagaku Kaishi*, 761 (1977).
- Hamzaoui, H., and Batis, H., *J. Chim. Phys.* **89**, 111 (1992).
- La Ginestra, A., Patrono, P., Berardelli, M. L., Galli, P., Ferragina, C., and Massucci, M. A., *J. Catal.* **103**, 346 (1987).
- Clearfield, A., and Thakur, D. S., *Appl. Catal.* **26**, 1 (1986).
- Cheng, S., Wang, J.-T., and Lin, C. L., *J. Chin. Chem. Soc.* **38**(6), 529 (1991).
- Hattori, H., in “Studies in Surface Science and Catalysis” (M. Guisnet, J. Barbier, J. Barrault, C. Bouchoule, D. Duprez, G. Perot, and C. Montassier, Eds.), Vol. 78, p. 35. Elsevier, Amsterdam, 1993.
- Conanec, R., Marchand, R., and Laurent, Y., *High Temp. Chem. Processes* **1**, 157 (1992).
- Gandia, L. M., Malm, R., Conanec, R., Marchand, R., Laurent, Y., and Montes, M., *Appl. Catal. A* **114**, L1 (1994).
- Grange, P., Bastians, Ph., Conanec, R., Marchand, R., and Laurent, Y., *Appl. Catal. A* **114**, L191 (1994).
- Massinon, A., Odriozola, J. A., Bastians, Ph., Conanec, R., Marchand, R., Laurent, Y., and Grange, P., *Appl. Catal. A* **137**(1), 9 (1996).
- Grange, P., Bastians, Ph., Conanec, R., Marchand, R., Laurent, Y., Gandia, L., Montes, J., Fernandez, M., and Odriozola, J. A., in “Preparation of Catalysts VI” (G. Poncelet, J. Martens, B. Delmon, P. A. Jacobs, and P. Grange, Eds.), p. 389. Elsevier, Amsterdam, 1994.
- Marchand, R., Laurent, Y., Guyader, J., L’Haridon, P., and Verdier, P., *J. Eur. Ceram. Soc.* **8**, 197 (1991).
- Volpe, L., and Boudart, M., *J. Solid State Chem.* **59**, 332 (1985).
- Oyama, S. T., Schlatter, J. C., Metcalfe, J. E., and Lambert, J. M., *Ind. Eng. Chem. Res.* **27**, 1639 (1988).
- Guéguen, E., Kartheuser, B., Conanec, R., Marchand, R., Laurent, Y., and Grange, P., in “Catalysis on Solid Acids and Bases” (J. Weitkamp and B. Lücke, Eds.), Vol. 9601, p. 235. DGMK-Tagungsbericht, 1996.

18. Fripiat, N., and Grange, P., *J. Chem. Soc. Chem. Commun.*, **1409** (1996).
19. Wiame, H., Bois, L., L'Haridon, P., Laurent, Y., and Grange, P., *J. Eur. Ceram. Soc.*, in press.
20. Courty, Ph., Ajot, H., Marcilly, Ch., and Delmon, B., *Powder Technology* **7**, 21 (1973).
21. Fripiat, N., Conanec, R., Marchand, R., Laurent, Y., and Grange, P., *J. Europ. Ceram. Soc.*, in press.
22. Grekov, F. F., Guyader, J., Marchand, R., and Lang, J., *Rev. Chim. Min.* **15**, 341 (1978).
23. Rebenstorf, B., Lindblad, T., and Andersson, L. T., *J. Catal.* **128**, 293 (1991).
24. Yamaguchi, T., *Bull. Chem. Soc. Jpn.* **51**(9), 2482 (1978).
25. Moffat, J. B., *Catal. Rev. Sci. Eng.* **18**(2), 199 (1978).
26. Knözinger, H., *Adv. Catal.* **25**, 199 (1976).
27. Parry, E. P., *J. Catal.* **2**, 371 (1963).
28. Carniti, P., Gervasini, A., and Auroux, A., *J. Catal.* **150**, 274 (1994).
29. Lednor, P. W., *Catal. Today* **15**, 243 (1992).
30. Corma, A., Fornés, V., Martin-Aranda, R. M., and Rey, F., *J. Catal.* **134**, 58 (1992).